Spreading of miscible liquids

Daniel J. Walls,[1] Simon J. Haward,[2] Amy Q. Shen,[2] and Gerald G. Fuller[1,*]
[1]*Department of Chemical Engineering, Stanford University, Stanford, California 94305, USA*
[2]*Micro/Bio/Nanofluidics Unit, Okinawa Institute of Science and Technology Graduate University, 1919-1 Tancha, Onna-son, Kunigami-gun, Okinawa 904-0495, Japan*
(Received 21 January 2016; published 31 May 2016)

Miscible liquids commonly contact one another in natural and technological situations, often in the proximity of a solid substrate. In the scenario where a drop of one liquid finds itself on a solid surface and immersed within a second, miscible liquid, it will spread spontaneously across the surface. We show experimental findings of the spreading of sessile drops in miscible environments that have distinctly different shape evolution and power-law dynamics from sessile drops that spread in immiscible environments, which have been reported previously. We develop a characteristic time to scale radial data of the spreading sessile drops based on a drainage flow due to gravity. This time scale is effective for a homologous subset of the liquids studied. However, it has limitations when applied to significantly chemically different, yet miscible, liquid pairings; we postulate that the surface energies between each liquid and the solid surface becomes important for this other subset of the liquids studied. Initial experiments performed with pendant drops in miscible environments support the drainage flow observed in the sessile drop systems.

DOI: 10.1103/PhysRevFluids.1.013904

I. INTRODUCTION

The spreading of miscible liquids is encountered in many important natural and technological processes. In the human body, miscible liquids continuously come into contact with one another and a prominent example is mucous interacting with other bodily fluids. An important technological problem is the manner in which spilled oil can spread across the bodies of animals coated with body oils [1,2]. Another example is the common occurrence of rinsing personal products from the body.

The spreading of liquids is a classic problem in interfacial fluid mechanics, involving a system of three phases: the spreading liquid, the substrate across which it spreads, and the ambient fluid in which both are enveloped. Here, the ambient fluid can be either a gas or a liquid.

Figure 1 depicts a spreading liquid that has formed a sessile drop. If this shape is at equilibrium, the sessile drop will form a contact angle, θ_E, given by Young's equation:

$$\sigma_{\mathrm{LF}} \cos\theta_E = \sigma_{\mathrm{SF}} - \sigma_{\mathrm{SL}}, \tag{1}$$

where the three coefficients σ_{LF}, σ_{SF}, and σ_{SL} are the surface energies at the liquid-fluid (LF), solid-fluid (SF), and solid-liquid (SL) interfaces, respectively.

Often, the spreading of liquids is studied in the context of sessile drops, as they naturally arise as either equilibrium or transitory states. When a sessile drop is in a transitory state, the spreading liquid will adjust its shape and contact angle to move towards equilibrium. The manner in which a sessile drop spreads in an immiscible fluid has been reported previously [3–12]. Sessile drops in air with finite initial contact angles, yet with equilibrium contact angles of zero, have been measured to spread with well-known power-law dependencies in time. Here, the power-law index depends on whether fluid flow is driven either by gravity or by capillarity, which can be determined by calculating the Bond number, Bo, of the drop:

$$\mathrm{Bo} = \frac{\Delta\rho g R_o^2}{\sigma_{\mathrm{LF}}}, \tag{2}$$

*Corresponding author: ggf@stanford.edu

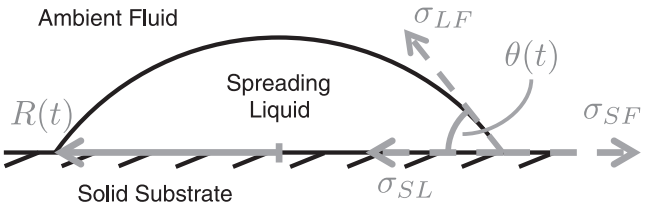

FIG. 1. Solid-liquid-fluid system and the force balance of the three surface energies—σ_{LF}, σ_{SF}, and σ_{SL}—arising at the three-phase contact line. The three subscripts indicate the surface energies at the solid-fluid (SF), solid-liquid (SL), and liquid-fluid (LF) interfaces. θ is the contact angle that the spreading liquid forms with the solid substrate. R is the radius of the spreading liquid. Both θ and R can be time-dependent parameters if the spreading liquid is not at its equilibrium shape.

where $\Delta\rho$ is the density difference between the spreading liquid and ambient fluid, g is acceleration due to gravity, and R_o is the initial radius of the spreading liquid. When Bo $\gg 1$, gravitational forces dominate the spreading dynamics; Bo $\ll$ 1 indicates that capillarity dominates. The radius of the spreading sessile drop follows a power law in time of $R \sim t^{1/8}$ in the gravity-dominated regime [5]. The regime, where the spreading of a sessile drop occurs due to the action of capillary forces, is known as Tanner's law [6] and the radius of the drop propagates across the surface with a time dependence of $R \sim t^{1/10}$.

Eddi *et al.* investigated the early time dynamics of a spherical, viscous drop as it first comes into contact with a solid substrate [12]. They studied the advancement of the contact line as the drop spread in air and found that it follows a power law in time, where $R \sim t^{1/2}$ at short times. Interestingly, they found that the early spreading dynamics bore great similarity to the progression of the neck that develops between two coalescing drops [13]. Spreading is important in the application of concrete mixing as well. The spreadability of concrete has been gauged through a slump test, which measures the decrease in height of a conical frustum of fresh concrete over time as it slumps due to gravity [14,15].

This paper is concerned with the spreading of sessile drops that find themselves immersed within a second, miscible liquid. Additionally, observations of the shape evolution of pendant drops existing in a miscible environment are presented to support the study of miscible, sessile drops. To our knowledge, these problems have not been reported previously in the literature. A sessile drop in a miscible environment will spread spontaneously, and it is expected that, likewise, a pendant drop will continue to evolve in shape as a function of time. Sessile drops spread in an immiscible environment due to gravitational, capillary, or, potentially, Marangoni flows, all of which are possible for a sessile drop in a miscible environment, with an additional flux across the liquid-liquid interface that arises from diffusion due to the chemical potential difference between the two initially distinct, homogenous liquids. The fluid-fluid interface that merely translated with a spreading drop in an immiscible system now becomes less distinct in time as the two miscible liquids diffuse across their mutual boundary. Diffusion imparts a time dependence to the properties of the liquids in the diffusive region—notably the density, viscosity, and interfacial tension—that influence the spreading behavior. The relative importance of gravity, capillarity, and Marangoni stresses to a sessile drop in a miscible environment needs to be determined in order to understand how the spreading of such a drop occurs.

Both the existence and the magnitude of interfacial tension between miscible liquids have been studied in the past. The chemical potentials of two distinct liquids are different, even if they are completely miscible, and some finite interfacial tension can exist, even if small. Any such tension is expected to diminish in time as diffusion proceeds. One cause of the uncertainty surrounding interfacial tension is the inherent difficulty in measuring interfacial tension between miscible liquids. Establishing an initial condition consisting of a distinct, stationary liquid-liquid interface in the absence of perturbations is challenging.

Mason and his colleagues conducted measurements of the interfacial tension between two silicone oils using a Wilhelmy balance. The device was first loaded with the denser, more viscous of the two

silicone oils and allowed to equilibrate. Then the less dense, less viscous silicone oil was poured on top of the other. The act of establishing the initial condition induced convection into the two liquids, causing errors in measurements [16]. Kojima *et al.* performed drop impact studies as corn syrup droplets fell into bodies of water; they coupled the experiments with theoretical work. In order to rectify the developed theory with their observations, a finite value for interfacial tension needed to be introduced [17].

Pojman and his colleagues performed interfacial tension measurements for a few miscible liquid systems using a spinning-drop tensiometer. Using this technique, they were able to measure interfacial tensions several orders of magnitude less than the measurements performed by Mason with a Wilhelmy balance. They also noticed that the interfacial tension diminishes in time [18,19]. Lacaze *et al.* employed light scattering, another technique able to measure small interfacial tensions, on an isobutyric acid (IBA)–water system, also studied by Pojman. With this technique and liquid pairing, Lacaze *et al.* also observed interfacial tensions that diminished in time [20]. Stevar and Vorobev conducted experiments with several miscible liquid pairs using horizontal, square capillary tubes. The tube was first loaded with one liquid and then immersed in the second, miscible liquid. In time, the liquid-liquid interface moves as the first liquid flows out of the capillary tube, displaced by the second liquid. The authors note that the liquid-liquid interface moved with a speed proportional to $t^{-2/3}$ as the system evolved [21].

Borcia and co-workers performed experiments with two adjacent sessile drops in air, each composed of a different, yet miscible, liquid, and observed a delay in the coalescence of the two drops when the two contact lines were brought into contact tangentially. When this experiment was repeated with both drops comprised of identical liquids, coalescence occurred without delay. This difference in behavior was interpreted as verifying the existence of a finite interfacial tension existing between the two different, but miscible, liquids [22,23].

Nonetheless, we expect any observed evolution of miscible sessile and pendant drops to be primarily governed by gravitational forces but also influenced by the surface energies of the liquid and solid phases. Capillary forces and Marangoni stresses are likely to be of secondary importance due to the very small surface tensions that exist between miscible liquids. This assertion is supported both by calculations of very large Bond numbers in our experiments using estimates for interfacial tension from the work of Mason [16], Kojima [17], Pojman [18,19], and Lacaze [20], and through the observations described below. We aim to describe the fluid-mechanical mode of the spreading of sessile drops in miscible environments and the time evolution of that spreading through a series of experiments involving several pairs of miscible liquids and various imaging techniques, including particle tracking velocimetry (PTV) and confocal microscopy.

II. EXPERIMENT

A. Miscible sessile drop apparatus

An apparatus was developed to perform measurements of the evolution of both sessile and pendant drops in a miscible environment. It is displayed in Fig. 2 in the configuration for studying the spreading of sessile drops.

Solid substrates were cut from glass slides into 30-mm-diam discs. Surfaces were used untreated or modified by applying a solution of 1/30 (v/v) dimethyldichlorosilane (DDS)/hexane (Sigma-Aldrich, Silanization solution I) for 1 h. Untreated surfaces are referred to as hydrophilic glass surfaces; surfaces treated with the silane solution are referred to as hydrophobic glass surfaces. The circular disks were affixed to a thin metal rod and suspended above the bath of the ambient liquid. The container holding the ambient liquid was constructed by bonding five glass slides to form a 50-mm cube and rested on a vertical stage that translates to immerse the substrate.

Cameras are mounted to observe spreading from side and bottom perspectives. Backlighting for both cameras was projected through telecentric lenses to collimate light and best distinguish the liquid-liquid interface. The bottom camera best serves the purpose of visualizing the contact line of

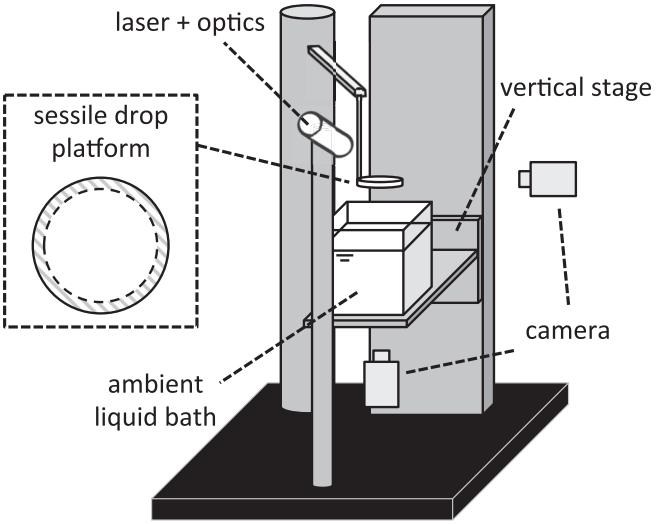

FIG. 2. Experimental setup for performing sessile drop experiments. First, a sessile drop is formed in air on a circular disk, which serves as the sessile drop platform. The circular disk is affixed to a thin metal rod and suspended above a bath of the ambient liquid. The bath of ambient liquid is set upon a platform mounted to a vertical stage that can translate in order to immerse the circular disk and sessile drop to initiate the miscible sessile drop spreading experiment. Cameras are positioned to image the spreading process from the side and below. A laser and cylindrical lens are mounted to produce a sheet of light orthogonal to the side camera to allow for PTV. The setup can accommodate pendant drop experiments by replacing the sessile drop platform with a fixture to hold a syringe needle. Inset: The pattern formed on a substrate for use in sessile drop experiments. There are two regions on each substrate, demarcated by the dashed circle. The first region is solid white, contained within the dashed circle, and the second exists between the dashed circle and the outer edge, striped gray and white. The diameter of the substrate is 30 mm and the width of the outer region is 2 mm. In the case of a hydrophilic surface, the interior, solid white region was protected to remain hydrophilic while the exterior, gray striped region was exposed to a hydrophobic treatment. In the alternate case of a hydrophobic surface, the interior region was exposed to a hydrophobic treatment while the exterior region was protected to remain hydrophilic. Patterning in such a way facilitated a symmetric immersion process.

the sessile drop, whereas the side camera enables the tracking of the leading-edge radius. When an immiscible drop spreads, these two features are identical. However, as seen below, this coincidence is not the case for the spreading of miscible drops.

Establishing the initial condition where a spreading liquid suddenly finds itself surrounded by a miscible environment is challenging. The experimental apparatus and immersion procedure were designed and refined to establish the initial condition of a miscible sessile drop with as little induced convection and deformation of the sessile drop as possible. First, the surface of the ambient liquid bath was raised to the height of the solid substrate. Then, the bath was raised an additional 5 mm at 1 mm/s to immerse the drop. During the immersion process, it is desirable that the ambient liquid wets the substrate and contacts the spreading liquid with radial symmetry.

The substrate surfaces were patterned, as shown in the inset of Fig. 2, to facilitate a symmetric immersion process. For a hydrophilic surface, a thin strip with a thickness of 2 mm around the edge of the disk was exposed to the silane solution to produce a hydrophobic treatment while the remainder of the disk was protected and remained hydrophilic. In the case of a hydrophobic surface, the reverse was performed: the interior region of the disk was exposed to the silane solution to produce a hydrophobic treatment while protecting a thin strip around the edge of the disk, which remained hydrophilic. The selection of liquid pairs was tailored such that the viscosity of the spreading liquid was greater than that of the ambient liquid to minimize the deformation of the drop during immersion.

TABLE I. Properties of the experimental liquids.

Liquid	Spreading or Ambient	Density (g/ml)	Viscosity (mPa s)	Contact angle in air (hydrophilic surface) (deg)	Contact angle in air (hydrophobic surface) (deg)	Surface tension (mN/m)
5 cSt silicone oil	Ambient	0.918	4.59	<5	<5	19.7
10 cSt silicone oil	Both	0.935	9.35	<5	<5	20.1
20 cSt silicone oil	Spreading	0.950	19.0	<5	<5	20.6
50 cSt silicone oil	Spreading	0.960	48.0	10	6	20.8
100 cSt silicone oil	Spreading	0.966	96.6	10	8	20.9
200 cSt silicone oil	Spreading	0.968	194	10	9	21.0
500 cSt silicone oil	Spreading	0.971	486	13	11	21.1
1000 cSt silicone oil	Spreading	0.971	971	15	11	21.2
5000 cSt silicone oil	Spreading	0.975	4880	15	14	21.3
10 000 cSt silicone oil	Spreading	0.975	9750	19	22	21.5
Corn syrup	Spreading	1.386	7000	60	100	66.5
Glycerol	Spreading	1.261	934	18	96	62.5
Water	Ambient	0.997	0.890	7	96	72.0
Tricresyl phosphate	Spreading	1.143	3.000	30	44	40.9
Ethanol	Ambient	0.789	1.074	<5	20	22.0
Isopropanol	Ambient	0.781	2.040	<5	14	20.9

Liquids used for sessile drops were silicone oils (Clearco Products; 10, 20, 50, 100, 200, 500, 1000, 5000, and 10 000 cSt pure silicone fluids), corn syrup (Karo; light corn syrup), glycerol (Alfa Aesar; ultrapure HPLC), and tricresyl phosphate (Aldrich; 90% grade). Silicone oil sessile drops were paired with ambient liquids of lower-viscosity silicone oils (5, 10 cSt). Corn syrup and glycerol sessile drops were paired with deionized water (Milli-Q Academic A10). Glycerol and tricresyl phosphate sessile drops were paired with ethanol (Fisher; anhydrous) and isopropanol (Fisher; HPLC). The volatility of the ambient liquids is not influential to the experiment, as the ambient-air interface is sufficiently far from the ambient-spreading interface of the drops. The density, viscosity, contact angles on the hydrophilic and hydrophobic surfaces in air, and surface tension for each liquid are displayed in Table I. The series of silicone oils used in this study was chosen by the similar surface tensions, which strengthens our expectation that the series is a homologous one with respect to the surface energy interaction of each silicone oil with the substrates.

The volumes of the sessile drops were varied between 1 and 20 μL without observing a change in the spreading behavior. Results presented here were gathered from experiments where the volume of the sessile drops was 5 μL.

B. Particle tracking velocimetry

A laser and glass cylindrical lens were added to the apparatus for the purposes of performing PTV experiments. A diode laser (OZ Optics) at 650 nm was split into a line with the glass cylindrical lens. The laser and cylindrical lens were aligned with the plane that intersected the meridian of the sessile drop orthogonal to the side camera, which is detailed in the schematic presented in Fig. 2. Microsphere particles were added to the drop liquid to scatter the light from the laser for imaging purposes. All particle imaging experiments were performed with the spreading liquid containing 6-μm microspheres at a concentration of 10^{-3} g/ml (ThermoScientific; Fluoro-Max green polystyrene microspheres). Velocity vectors were obtained by tracking the motion of individual particles in successive frames.

C. Confocal microscopy

Confocal microscopy experiments were performed using a Zeiss LSM 5 Live inverted confocal microscope. To fit the experiment within the geometry of the microscope, an alternate test chamber was needed. A 50 mm (l) × 50 mm (w) × 25 mm (h) glass box was constructed from five glass microscope slides and a 24-mm-diam hole was cut into the base of the box. A circular 25-mm No. 2 glass coverslip was then mounted over the hole to serve as the sessile drop substrate. The surface of the coverslip could be either hydrophilic or hydrophobic. A capillary tube was adhered to the top corner of the box, to which a syringe was attached to immerse the sessile drop in a miscible liquid. The volume of sessile drops for the confocal experiments was 1 μL. All confocal experiments were performed with the spreading liquid containing 0.2-μm microspheres at a concentration of 10^{-3} g/ml (Life Technologies; FluoSpheres yellow-green polystyrene microspheres).

The confocal microscope was programmed to scan across an XYZ volume that coincided with a radius of the sessile drop. A stack of images obtained in the Z direction from scans in the XY plane was reconstructed into one RZ plane image. A series of reconstructed images was gathered to illustrate how a cross section of the drop in the RZ plane behaves in time.

D. Miscible pendant drop apparatus

The apparatus from Fig. 2 can be modified to observe pendant drops by replacing the sessile drop platform with a syringe. Pendant drop experiments were performed for the two highest viscosity ratio pairs: (1) corn syrup and water, and (2) 10 000 cSt silicone oil and 5 cSt silicone oil. Experiments were performed with pendant drops of approximately 0.1 μL. Stainless-steel syringe needles (McMaster Carr) were used for the corn syrup and water system. PTFE-lined stainless-steel syringe needles (McMaster Carr) were used for the silicone oil system.

III. RESULTS AND DISCUSSION

A. Miscible sessile drop experiments

We have observed that a sessile drop spreading in a miscible environment progresses through a distinctly different shape evolution as compared to one present in an immiscible environment, such as air. Figure 3 shows a snapshot in time from the side and bottom perspectives of a corn syrup sessile drop spreading across a hydrophobic glass surface while immersed in water. The portion of the drop that leads its advancement is elevated above the liquid-solid interface (black arrows in Fig. 3), followed by the three-phase contact line (white arrows in Fig. 3). We refer to the most radially advanced and elevated portion of the drop as the leading edge, and the portion of the drop that remains in contact with the solid substrate as the contact line. This occurrence is in stark contrast to the case of a sessile drop spreading in air, where the leading edge is coincident with the contact line.

Figure 4 shows an image sequence taken from the side camera of a 10 000 cSt silicone oil sessile drop immersed in 5 cSt silicone oil, spreading across a hydrophilic glass surface, and Fig. 5 shows an image sequence taken from the side camera of a corn syrup sessile drop immersed in water, spreading across a hydrophilic glass surface. In these two series of images, each drop develops an elevated leading edge, which then leads the spreading process as it propagates radially outward. Determining the position of the contact line from this vantage point is difficult. When observing the spreading process from below, the contact line is more readily apparent. In the case of the silicone oil system in Fig. 4, the contact line could not be located with sufficient precision after a short time due to the very small difference in refractive indices of the liquid pair. At short times when it is still visible, the contact line appears to remain stationary. For the corn syrup–water experiment in Fig. 5, the contact line moves outward, but at a slower rate than that of the leading edge.

PTV experiments were performed with the spreading liquid containing 6-μm-diam microsphere particles at a concentration of 10^{-3} g/ml to visualize the flow pattern that develops within the miscible sessile drop system. Figure 6 shows an image from a PTV experiment of a corn syrup sessile drop immersed in water and spreading across a hydrophobic glass surface. The arrows indicate

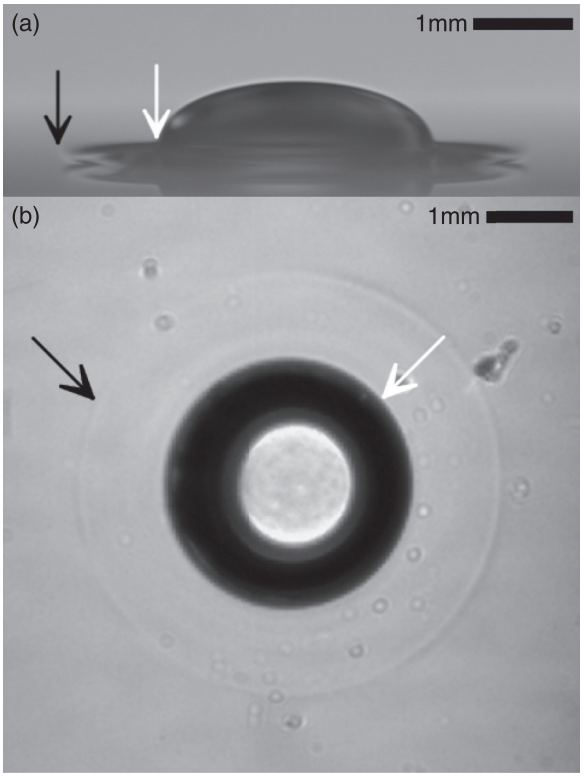

FIG. 3. Snapshot of a corn syrup sessile drop spreading while immersed in water as visualized from the (a) side and (b) bottom. The black arrows indicate the most radially advanced portion of the drop, which is elevated above the solid surface, and we refer to it as the leading edge. The white arrows indicate the most radially advanced portion of the drop that remains in contact with the solid surface, and we refer to it as the contact line. The shape evolution for this sessile drop immersed in a miscible environment is distinctly different from that of one present in an immiscible environment. Refer to the Supplemental Material [24] for the full movie from which these frames were taken.

velocity vectors obtained from particle movement. Motion was largely restricted to the liquid-liquid interface and particles away from the interface do not move significantly. The interfacial region, where the viscosity is intermediate between water and corn syrup, drains downward and feeds into the leading-edge portion of the drop. As this drainage continues, the height of the drop decreases and the liquid-liquid interface moves downward. As the liquid-liquid interface descends, particles located within the drop are continually exposed to the interface and are carried within the thin drainage flow of the boundary layer. This draining phenomenon was observed for the other liquid pairs as well; however, it is most clearly evident in this system due to the high viscosity ratio of the two liquids ($\mu_{spr}/\mu_{amb} \sim 8000$).

Figure 7 shows a reconstructed, side view image sequence from a confocal microscopy experiment of a corn syrup sessile drop immersed in water and spreading across a hydrophobic glass surface. A frustum of the sessile drop, its base coinciding with the glass surface, was scanned along a radial slice, as indicated in the top frame of the figure. From the image sequence, one can see the development of the elevated leading edge, first visible at 0.9 s here, and its subsequent motion. The leading edge, indicated by white arrows, propagates radially outward, coasting across the substrate while elevated above it, in the fashion of a plug flow, as a viscous liquid that moves through a relatively much lower viscosity medium. The thicknesses of the leading edge of the spreading drop and the ambient liquid

FIG. 4. A sequence of images taken over time of a 10 000 cSt silicone oil sessile drop immersed in 5 cSt silicone oil and spreading across a hydrophilic glass surface. In each frame, the upper, light region is the ambient liquid and the lower, dark region is the substrate. The sessile drop begins to spread by developing an elevated leading edge that leads the advancement of the drop across the surface. Refer to the Supplemental Material [24] for the full movie from which these frames were taken.

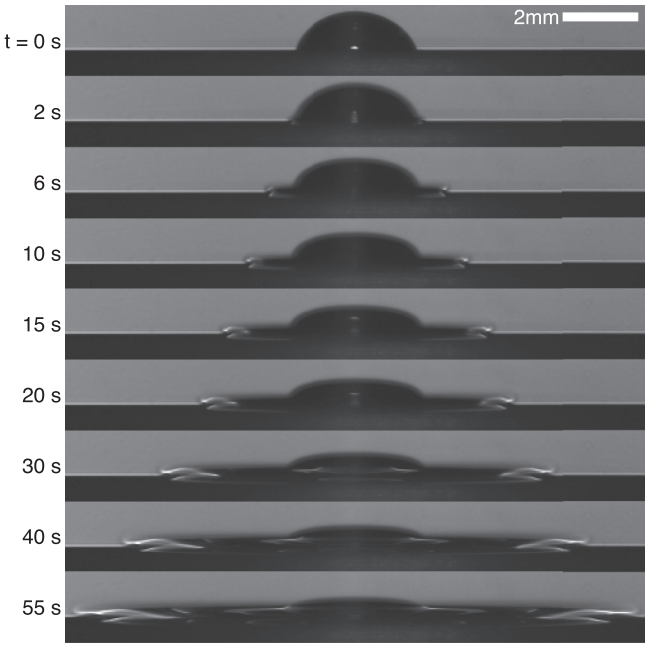

FIG. 5. A sequence of images taken over time of a corn syrup sessile drop immersed in water and spreading across a hydrophilic glass surface. In each frame, the upper, light region is the ambient liquid and the lower, dark region is the substrate. The sessile drop begins to spread by developing an elevated leading edge that leads the advancement of the drop across the surface. Refer to the Supplemental Material [24] for the full movie from which these frames were taken.

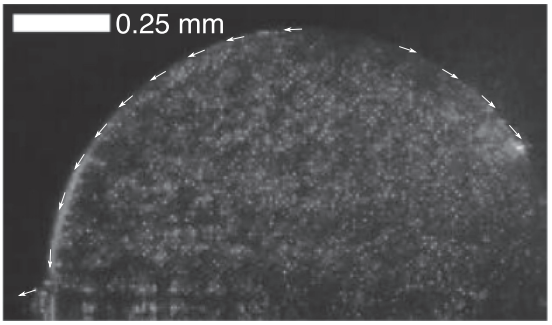

FIG. 6. Image from a PTV experiment of a corn syrup sessile drop immersed in water and spreading across a hydrophobic glass surface. The corn syrup contains 6-μm microspheres at a concentration of 10^{-3} g/ml, which scatter the incident laser light. The arrows indicate velocity vectors obtained from individual particle movement. Motion was largely restricted to the corn syrup–water interface and particles within the drop and away from the liquid-liquid interface remain stationary. Refer to the Supplemental Material [24] for the full movie from which this frame was taken.

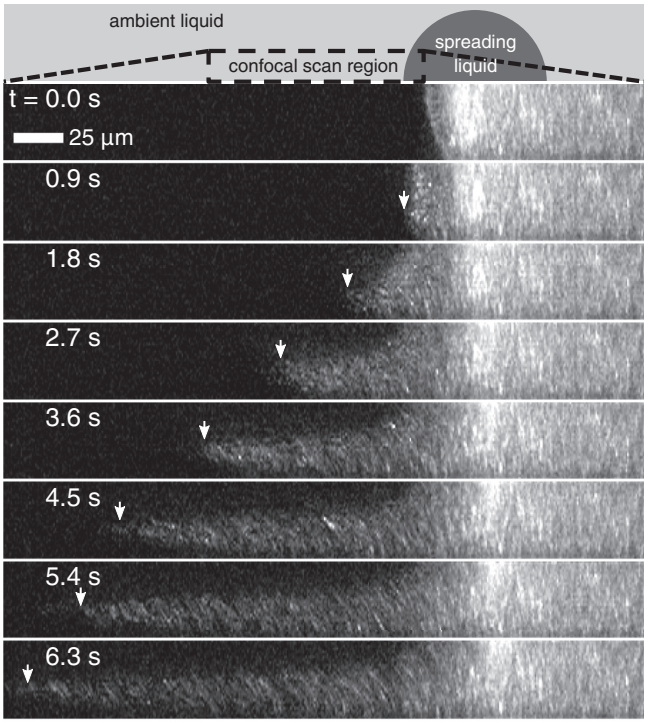

FIG. 7. Reconstructed, side view image sequence from a confocal microscopy experiment of a corn syrup sessile drop spreading across a hydrophobic glass surface while immersed in water. A frustum of the sessile drop, its base coinciding with the glass surface, was scanned along a radial slice, as displayed in the top frame. The corn syrup contains 0.2-μm fluorescent polystyrene microspheres at a concentration of 10^{-3} g/ml, while the water contains no fluorescent material. Thus, the corn syrup phase exists as the bright regions of the images and the water phase appears dark. One can see the development of the leading edge, first visible at 0.9 s here, and indicated by white arrows thereafter; it is elevated approximately 35 μm above the substrate at its tip after approximately 4.5 s. Refer to the Supplemental Material [24] for a movie of this image sequence.

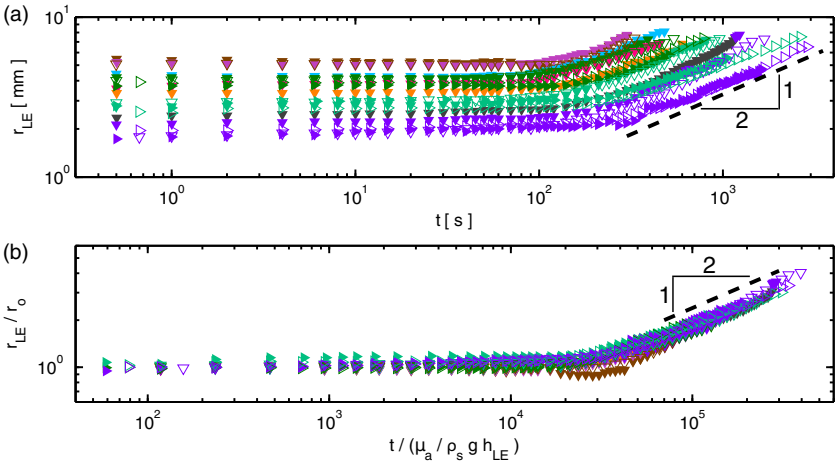

FIG. 8. Plots of leading-edge radius measurements as a function of time for homologous silicone oil pairs on hydrophilic and hydrophobic glass. (a) Unscaled data. (b) The leading-edge radius data are scaled by the initial radius of each sessile drop and time is scaled by a characteristic drainage time, $\tau = \mu_a/\rho_s g h_{\mathrm{LE}}$, where μ_a is the viscosity of the ambient liquid, ρ_s is the density of the spreading liquid, g is the acceleration due to gravity, and h_{LE} is the thickness of the elevated leading edge. The dashed line in each plot represents a square-root power law, which is a time dependence indicative of a diffusion process. Symbol shape and color are coded for the ambient and spreading liquids, respectively. Symbol shapes ▼ and ▶ indicate the ambient liquids are 5 cSt and 10 cSt silicone oils, respectively. Symbol colors ■, ■, ■, ■, ■, ■, ■, ■, and ■ indicate the spreading liquids are 10, 20, 50, 100, 200, 500, 1000, 5000, and 10 000 cSt silicone oils, respectively. Solid and open symbols ▼ and ▽ represent experiments performed with 10 cSt silicone oil as the spreading liquid and 5 cSt silicone oil as the ambient liquid on hydrophilic and hydrophobic surfaces, respectively. One experimental pair exhibits an initial retraction of the radius prior to spreading outward following a square-root power law in time. Refer to the Supplemental Material [24] for a series of images and movie for this particular experiment.

that resides below can be measured. At its tip, the leading edge is elevated approximately 35 μm above the solid surface. Confocal microscopy experiments were performed for other liquid pairs as well and showed similar behavior in the development of an elevated leading edge.

Figure 8(a) shows a plot of the leading-edge radius measurements as a function of time for the homologous silicone oil pairs on hydrophilic and hydrophobic glass surfaces. There is a variation in the initial radii of the drops, partially due to slight differences in the volume of the sessile drops, but primarily due to the different contact angles that each spreading liquid forms on the substrates in air. At the small contact angles that each silicone oil forms on the surfaces, small variations in these contact angles produce relatively larger changes in radius. It appears that at some point in the spreading process, each liquid pairing approaches a similar power law in time. A dashed reference line is plotted alongside the data representing a square-root power law, which is a time dependence indicative of a diffusion process.

If we scale the leading-edge radius and time data presented in Fig. 8(a) by the initial drop radius and a characteristic drainage time, respectively, the plot shown in Fig. 8(b) is obtained. Scaling the leading-edge radius by the initial radius of each sessile drop collapses the vertical axis. When the horizontal axis (time) is scaled by a characteristic drainage time, the data also largely collapse to reveal a power-law response of the leading edge that closely follows a square-root dependence in time, which is reminiscent of a diffusive process. The characteristic drainage time, τ, is calculated as follows:

$$\tau = \frac{\mu_a}{\rho_s g h_{\mathrm{LE}}} \tag{3}$$

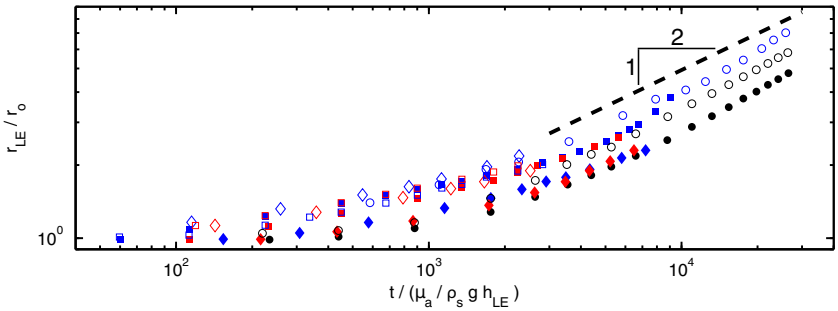

FIG. 9. Plot of leading-edge radius measurements as a function of time for pairs of nonhomologous liquids on hydrophilic and hydrophobic glass surfaces. The leading-edge radius data are scaled by the initial radius of each sessile drop and time is scaled by a characteristic drainage time, $\tau = \mu_a/\rho_s g h_{\mathrm{LE}}$, where μ_a is the viscosity of the ambient liquid, ρ_s is the density of the spreading liquid, g is the acceleration due to gravity, and h_{LE} is the thickness of the elevated leading edge. The dashed line is plotted alongside the data representing a square-root power law, which is a time dependence indicative of a diffusion process. Symbol shape and color are coded for the ambient and spreading liquids, respectively. Symbol shapes, ●, ♦, and ■ indicate the ambient liquid as water, ethanol, or isopropanol, respectively. Symbol colors ■, ■, and ■ indicate the spreading liquid as corn syrup, glycerol, or tricresyl phosphate, respectively. Solid and open symbols ● and ○ represent experiments performed with corn syrup as the spreading liquid and water as the ambient liquid on hydrophilic and hydrophobic surfaces, respectively.

where μ_a is the viscosity of the ambient liquid, ρ_s is the density of the spreading (drop) liquid, and h_{LE} is the thickness of the elevated leading edge. Bhamla *et al.* derived a similar time scale previously for a thin liquid film draining from a curved, solid substrate [25]. Here, the thin liquid film is a mixture of the ambient and spreading liquids and drains from the sessile drop in the presence of the ambient liquid. The viscosity of a viscous fluid decreases significantly and nonlinearly with the introduction of a small quantity of diluent and towards the viscosity of the diluent. Density is less responsive with the introduction of a diluent, and decreases more linearly [26]. It is expected that the viscosity and density of the draining liquid can be represented best by the viscosity of the ambient liquid and density of the spreading liquid, respectively. We use the thickness of the elevated leading edge of the spreading liquid, h_{LE}, as the characteristic length scale of the problem. As evidenced by the confocal and PTV experiments, this thickness is representative of the thickness of the draining region along the liquid-liquid interface, as one liquid flows into the other and propagates in the fashion of a plug flow.

The silicone oil data displayed in Fig. 8(a) can be collapsed onto the master curve displayed in Fig. 8(b), independent of consideration of the influence of the solid substrates. This observation is not surprising given the fact that the silicone oil series was chosen as a homologous set and one would expect that similar surface interactions would exist between the silicone oils within a pair and the substrates considered. As seen below for the nonhomologous liquid pairs, the simple scaling introduced in Fig. 8(b) is no longer sufficient.

Figure 9 shows a plot of the leading-edge radius measurements as a function of time for miscible, nonhomologous liquid pairs on hydrophilic and hydrophobic glass surfaces. The leading-edge radius data are scaled by the initial radius of each sessile drop and time is scaled by the characteristic drainage time presented in Eq. (3). The scaled data presented in Fig. 9 do not exhibit a collective response like that of the data displayed in Fig. 8(b), obtained using homologous silicone oil liquid pairs. However, after some initial development period, the leading edge for all liquid pairs exhibits a power-law response closely following a square-root dependence in time. The failure to collapse the data for pairs of nonhomologous liquids when scaling solely by a characteristic drainage time may be due to the different surface energies of each liquid to the solid substrate within a pair.

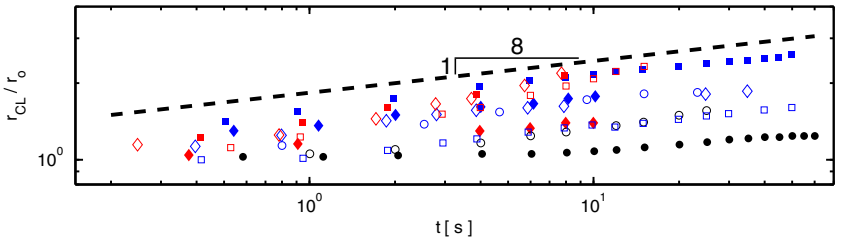

FIG. 10. Plot of contact-line radius measurements as a function of time for liquid pairs not involving silicone oils on hydrophilic and hydrophobic glass surfaces. The contact-line radius data are scaled by the initial radius of each sessile drop and time is left unscaled. The dashed line is plotted alongside the data representing a power law of $t^{1/8}$. Symbol shapes ●, ♦, and ■ indicate the ambient liquids are water, ethanol, and isopropanol, respectively. Symbol colors ■, ■, and ■ indicate the spreading liquids are corn syrup, glycerol, and tricresyl phosphate, respectively. Solid and open symbols ● and ○ represent experiments performed with corn syrup as the spreading liquid and water as the ambient liquid on hydrophilic and hydrophobic surfaces, respectively.

One might expect that differences in these surface energies within a pair could influence the time scale for a sessile drop to develop an elevated leading edge and commence spreading. Furthermore, the homologous series of silicone oils would be expected to have similar surface energies, at least much closer in value than substantially chemically different, yet miscible, liquids, which may explain why the scaling is more effective for the former.

Figure 10 shows a plot of contact-line radius measurements as a function of time for miscible liquid pairs not involving silicone oils on hydrophobic and hydrophilic glass surfaces. The contact-line radius data are scaled by the initial radius of each sessile drop and time is left unscaled. A scaling for the horizontal axis (time) has not been found to reveal a collective response of the data. As noted previously from observation of the shape evolution of the drops, the contact line advances more slowly than the elevated leading edge. This observation is apparent in the quantification of the contact-line movement in time for the experiments in Fig. 10. No experiment shows a contact line that spreads exceeding a power law in time of $t^{1/8}$, which is plotted as a dashed line alongside the data in Fig. 10, whereas the elevated leading edge follows a square-root power law after some initial development time. The power law of $t^{1/8}$ represents the growth in the radius of a sessile drop with a finite initial contact angle, spreading due to gravity in air across a surface on which it has an equilibrium contact angle of zero. Using the interfacial tensions determined by Mason [16], Kojima [17], Pojman [18,19], and Lacaze [20] as a range of estimates for the interfacial tension of the liquid pairings in Fig. 10, Bond numbers were calculated that indicate that each of these spreading liquids exists in the gravity-dominated spreading regime. Surface energies between each liquid and the solid substrate appear to be critical, as the contact-line radii of the spreading liquids studied here follow power laws below $t^{1/8}$, which change across the different surface treatments. However, a literature search for such surface energy information, either experiment or theory, provided no additional values.

B. Miscible pendant drop

In support of the experiments and findings related to the spreading of sessile drops in miscible environments, we conducted preliminary experiments for pendant drops in miscible environments. The images shown below provide additional evidence that a draining flow occurs at the liquid-liquid interface. The pendant drop experiments also eliminate the solid surface present for a sessile drop, which offers a route to circumvent the issue of unknown surface energies.

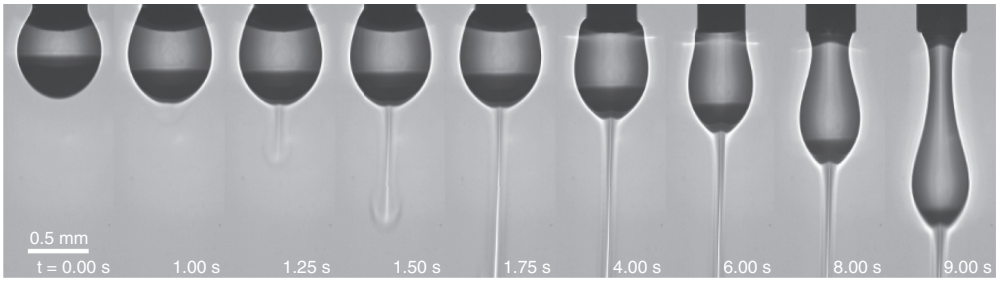

FIG. 11. Image sequence taken in time of a corn syrup pendant drop immersed in water. A strand emanates from the apex of the drop and continues to flow as the entire drop descends and elongates. Refer to the Supplemental Material [24] for the full movie from which these frames were taken.

Figure 11 shows a series of images taken of a corn syrup pendant drop immersed in water. At some time after immersion, a strand emanates from the apex of the drop and continues to flow downward. Eventually, the entire drop begins to descend and elongate.

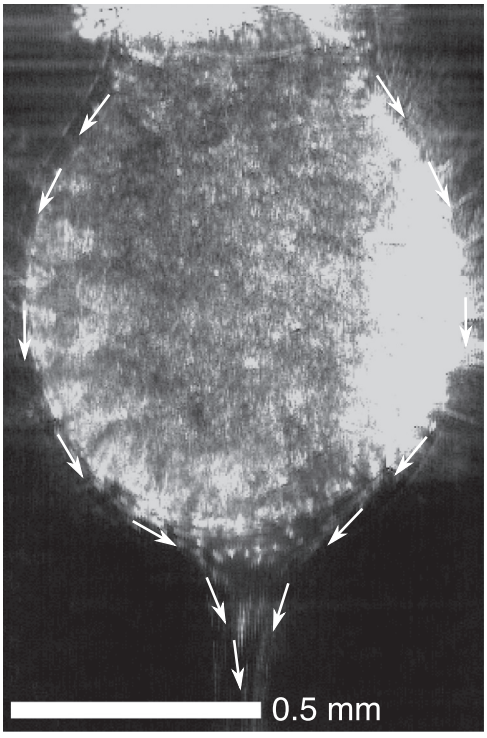

FIG. 12. Image from a PTV experiment of a corn syrup pendant drop immersed in water. The corn syrup contains 6-μm microspheres at a concentration of 10^{-3} g/ml, which scatter the incident laser light. The arrows indicate velocity vectors obtained from particle movement. Motion was largely restricted to the corn syrup–water interface. Particles within the pendant drop and away from the liquid-liquid interface move with the drop as it descends and elongates; within the reference frame of the pendant drop, these interior particles do not move significantly. Refer to the Supplemental Material [24] for the full movie from which this frame was taken.

Figure 12 shows an image from a PTV experiment of a corn syrup pendant drop in water. The arrows indicate velocity vectors obtained from individual particle movement. Motion was largely restricted to the liquid-liquid interface on the main body of the drop and to a thin liquid jet descending from the apex. Particles within the drop move only due to the descent of the drop itself as it elongates. As particles descend along the liquid-liquid interface, they reach the apex of the pendant drop and continue to flow downward in a thin strand. This behavior is remarkably similar in appearance to the findings of Garbin *et al.*, where a pendant drop of oil with its surface laden with nanoparticles and suspended in water was contracted and, at a critical size, shed the nanoparticles from its surface, resulting in a strand descending from the apex of the drop [27].

Pendant drop experiments were also conducted with 10 000 cSt silicone oil and 5 cSt silicone oil as the drop and ambient liquids, respectively. Similar behavior was observed to that of the corn syrup and water system shown in Figs. 11 and 12, where a strand emanated from the apex of the drop and fluid flow was restricted to the liquid-liquid interface and the strand. A movie of this system is included in the Supplemental Material [24]. A more detailed investigation of the interaction of pendant drops with miscible environments is presently under way in our laboratory.

IV. CONCLUSIONS

A sessile drop immersed in a miscible environment undergoes a distinctly different shape evolution than one present in immiscible surroundings. A sessile drop spreading across a solid surface while immersed in a miscible environment develops an elevated leading edge in addition to its contact line. This elevated leading edge actually leads the radial advancement of the drop, and the contact line advances at a slower rate. Through experiments using particle imaging techniques—PTV and confocal microscopy—fluid motion of the miscible systems was visualized. PTV experiments revealed that fluid flow is largely restricted to the liquid-liquid interface between the drop and ambient surrounding, appearing as a draining flow that feeds into either the leading edge of a sessile drop or the descending strand of a pendant drop. Confocal microscopy of sessile drops captured images of the development and length scale of the leading edge. Measurements of the leading-edge radius as a function of time for sessile drop systems of silicone oils on two different surfaces were collapsed to a collective response by scaling leading-edge radial data with the initial radius of the sessile drop and time data by a characteristic drainage time. However, when applying the same scaling to the leading-edge radial data of the other liquid pairs, which are substantially chemically different, yet miscible (unlike the homologous silicone oil experiments), a single collective response was not observed across the different liquid pairs or the different surfaces. In light of this difference in scaling outcomes, we suspect that the difference in the surface energies existent between each liquid of a pair and the solid substrate is important for the substantially chemically different, yet miscible, liquid pairs, which is not considered in the scaling parameter. The disparity in the success of the scaling for these two sets of liquid pairs may indicate that the difference in these two surface energies for liquid pairs from the homologous series of silicone oils is negligible or zero, but nonzero and influential for the liquid pairs containing substantially chemically different, yet miscible, liquids. Regardless of these groupings, we observed across all liquid pairs studied that, after some initial development period, the growth of the leading-edge radius exhibits a power-law response closely following a square-root dependence in time. The propagation of the contact line of a sessile drop likewise appears to depend on the surface energies that exist between each liquid of the pair and the surface, as each liquid competes to wet the surface. Observations of pendant drops in miscible environments support the findings from the study pertaining to sessile drops that a drainage flow occurs at the miscible liquid-liquid interface.

ACKNOWLEDGMENTS

The authors are grateful for funding from NSF CBET Grant No. 1335632 (D.J.W., A.Q.S., G.G.F.) and the Stanford Graduate Fellowship in Science and Engineering (D.J.W.). We gratefully

acknowledge support from the OIST Graduate University with subsidy funding from the Cabinet Office, Government of Japan (S.J.H. and A.Q.S.). The authors would like to thank Shristi Singh for her assistance in performing sessile drop experiments and Cédric Espenel for his expertise in confocal microscopy.

[1] M. Swedmark, A. Granmo, and S. Kollberg, Effects of oil dispersants and oil emulsions on marine animals, Water Res. **7**, 1649 (1973).
[2] J. Geraci, *Sea Mammals and Oil: Confronting the Risks* (Elsevier Science, New York, 2012).
[3] C. Huh and L. E. Scriven, Hydrodynamic model of steady movement of a solid/liquid/fluid contact line, J. Colloid Interface Sci. **35**, 85 (1971).
[4] O. V. Voinov, Hydrodynamics of wetting, Fluid Dyn. **11**, 714 (1976).
[5] H. E. Huppert, The propagation of two-dimensional and axisymmetric viscous gravity currents over a rigid horizontal surface, J. Fluid Mech. **121**, 43 (1982).
[6] L. H. Tanner, The spreading of silicone oil drops on horizontal surfaces, J. Phys. D **12**, 1473 (1979).
[7] R. G. Cox, The dynamics of the spreading of liquids on a solid surface. Part 1. Viscous flow, J. Fluid Mech. **168**, 169 (1986).
[8] R. G. Cox, The dynamics of the spreading of liquids on a solid surface. Part 2. Surfactants, J. Fluid Mech. **168**, 195 (1986).
[9] J. Joanny and D. Andelman, Steady-state motion of a liquid/liquid/solid contact line, J. Colloid Interface Sci. **119**, 451 (1987).
[10] A. Cazabat, How does a droplet spread? Contemp. Phys. **28**, 347 (1987).
[11] L. M. Pismen and J. Eggers, Solvability condition for the moving contact line, Phys. Rev. E **78**, 056304 (2008).
[12] A. Eddi, K. G. Winkels, and J. H. Snoeijer, Short time dynamics of viscous drop spreading, Phys. Fluids **25**, 013102 (2013).
[13] D. G. A. L. Aarts, H. N. W. Lekkerkerker, H. Guo, G. H. Wegdam, and D. Bonn, Hydrodynamics of Droplet Coalescence, Phys. Rev. Lett. **95**, 164503 (2005).
[14] W. R. Schowalter and G. Christensen, Toward a rationalization of the slump test for fresh concrete: Comparisons of calculations and experiments, J. Rheol. **42**, 865 (1998).
[15] ASTM C143/C143M-15a, Standard Test Method for Slump of Hydraulic-Cement Concrete, ASTM International, West Conshohocken, PA, 2015, www.astm.org.
[16] P. G. Smith, T. G. M. van de Ven, and S. G. Mason, The transient interfacial tension between two miscible fluids, J. Colloid Interface Sci. **80**, 302 (1981).
[17] M. Kojima, E. J. Hinch, and A. Acrivos, The formation and expansion of a toroidal drop moving in a viscous fluid, Phys. Fluids **27**, 19 (1984).
[18] J. A. Pojman, C. Whitmore, M. L. T. Liveri, R. Lombardo, J. Marszalek, R. Parker, and B. Zoltowski, Evidence for the existence of an effective interfacial tension between miscible fluids: Isobutyric acid/water and 1-butanol/water in a spinning-drop tensiometer, Langmuir **22**, 2569 (2006).
[19] B. Zoltowski, Y. Chekanov, J. Masere, J. A. Pojman, and V. Volpert, Evidence for the existence of an effective interfacial tension between miscible fluids. 2. Dodecyl acrylate/poly(dodecyl acrylate) in a spinning drop tensiometer, Langmuir **23**, 5522 (2007).
[20] L. Lacaze, P. Guenoun, D. Beysens, M. Delsanti, P. Petitjeans, and P. Kurowski, Transient surface tension in miscible liquids, Phys. Rev. E **82**, 041606 (2010).
[21] M. S. P. Stevar and A. Vorobev, Shapes and dynamics of miscible liquid/liquid interfaces in horizontal capillary tubes, J. Colloid Interface Sci. **383**, 184 (2012).
[22] R. Borcia, S. Menzel, M. Bestehorn, S. Karpitschka, and H. Riegler, Delayed coalescence of droplets with miscible liquids: Lubrication and phase field theories, Eur. Phys. J. E **34**, 24 (2011).

[23] S. Karpitschka and H. Riegler, Noncoalescence of Sessile Drops from Different but Miscible Liquids: Hydrodynamic Analysis of the Twin Drop Contour as a Self-Stabilizing Traveling Wave, Phys. Rev. Lett. **109**, 066103 (2012).

[24] See Supplemental Material at http://link.aps.org/supplemental/10.1103/PhysRevFluids.1.013904 for movies from which frames were taken to create Figs. 3–7; a movie and image sequence of a 10 cSt silicone oil sessile drop retracting on hydrophobic glass while immersed in 5 cSt silicone oil; and a movie of a pendant drop of 10 000 cSt silicone oil evolving while immersed in 5 cSt silicone oil.

[25] M. S. Bhamla, C. E. Giacomin, C. Balemans, and G. G. Fuller, Influence of interfacial rheology on drainage from curved surfaces, Soft Matter **10**, 6917 (2014).

[26] Glycerine Producers' Association, *Physical Properties of Glycerine and Its Solutions* (Glycerine Producers' Association, New York, 1963).

[27] V. Garbin, J. C. Crocker, and K. J. Stebe, Forced desorption of nanoparticles from an oil-water interface, Langmuir **28**, 1663 (2012).